STUDY OF RESISTANCE SPOT WELDING VIA EXPERIMENTAL, NUMERICAL AND ADVANCED ANALYTICAL METHODS

H. GAO, R. ZWART, E. VD AA, T. VD VELDT

Tata Steel in the Netherlands

DOI 10.3217/978-3-85125-968-1-11

ABSTRACT

In this work, finite element welding models are firstly validated with experimental measurements. Cases with different weld time, weld current and squeeze force are subsequently simulated in order to create a new database. Multiple linear regression, decision tree and random forest methods are used to train the analytical models. The trained analytical models are used to predict new experiments with reasonably good accuracy. In addition, weights for the input variables are explicitly ranked and discussed, which provides valuable information for optimizing the welding process. The main conclusions are summarized as follows,

- The approaches proposed in this work to combine the experiments, numerical models and analytical models are proven to be reliable and can be extended to other materials and processes.
- Increase in weld time or weld current, or decrease in squeeze force will increase the nugget size. With the studied material, multiple linear regression model provides two equations to calculate the nugget diameter and height with respect to weld time, weld current and squeeze force. Decision tree has a slightly better accuracy than multiple linear regression. Random forest provides the best predictions.
- Weld current has a dominating weight (more than 0.85) to determine the final nugget size. Squeeze force has a weight of 0.12 for determining the nugget height.

Key words: Resistance spot welding, Finite element model, Advanced analytics, AHSS

INTRODUCTION

Advanced high strength steels (AHSS) are increasingly used by the automotive manufacturers to reduce weight of a vehicle. A 10% reduction in vehicle weight can save fuel by 3% to 7% [1]. It has been reported that more than 4000 welds are made on a body in white car frame [2]. Resistance spot welding is the mostly applied method due to low cost, high degree of automation and small workload. The strength of a weld is strongly dependent on the weld nugget size. Therefore, it is of great importance to understand the relationship between the weld nugget size and welding parameters.

Finite element modelling is a widely used method to predict thermal and mechanical material responses during welding [3]. However, a virtual heat flux with a certain distribution has to be defined for simulation of either a laser welding or arc welding process [4-5], which always leads to a discussion on its reliability. Simulation of resistance spot welding can be fully based on the physics of Joule heating, where heat generation is calculated from the contact resistance at the sheet interface [6]. Therefore, combination of experimental and numerical approaches becomes an effective way to gain a better insight of temperature and strain/stress evolution during resistance spot welding and optimize welding parameters on demand. However, for a physical-based model with complex structure and processing conditions, calculation time for a numerical model can be very expensive. In addition, weights of input variables cannot be explicitly studied from simulation. Any changes in material properties, sample dimension and welding parameters will lead to a re-run of the model.

With development of modern high-speed computers, modeling based on big data has become a powerful approach to control and optimize different process parameters. Advanced analytical model has proven to an effective tool for resolving complex problems related to multiple factors [7]. Therefore, combination of experimental, numerical and advanced analytical methods to study resistance spot welding is explored in this work. An advanced high strength steel DP800-GI with a thickness of 1.2 mm was selected for resistance spot welding experiments. Finite element welding models are firstly constructed and validated with experimental measurements. A new database with different squeeze force, weld time and weld current are subsequently simulated. Multiple linear regression, decision tree and random forest methods are used to train the analytical models. The trained analytical models are used to predict new experiments with reasonably good accuracy. In addition, weights for the input variables are explicitly ranked and discussed, which provides valuable information for optimizing the welding process.

MATERIALS AND METHODS

MATERIAL AND WELDING EXPERIMENT

A dual phase (DP) steel with a thickness of 1.2 mm was selected for the experimental approaches in this study. This steel was received in a cold-rolled and galvanized condition with a coating weight of 50 gm−2. The testing coupons were prepared with a dimension of 45 mm x 45 mm. The chemical compositions of the studied material with Fe balanced are listed in Table 1.

Table 1 Chemical composition of studied material with Fe balanced (wt%)

C	Si	Mn	Al
0.15	0.096	2.063	0.647

Resistance spot welds were produced on a 1000 MHz MFDC spot welding machine, using a constant current regulation. ISO5821 F1-16-20-6 CuCr1Zr electrodes were tip-

dressed before use. The welding specification was according to the VDEh SEP1220-2 standard [8], as shown in Table 2. The welding current range was determined by producing two welds per current setting, starting from a welding current of 3.0 kA with an increment step of 0.2 kA. The minimum current was found when the weld spot diameter is greater than $4\sqrt{t}$ (t refers to sample thickness). When splash occurs between the sheets in two subsequent welds at identical welding current settings, the welding current was decreased in steps of 0.1 kA. The maximum current was determined until three consecutive welds were made without splash.

Table 2 Welding specification according to SEP1220-2

Force (kN)	Squeeze time (ms)	Weld time (ms)	Hold time (ms)
4	400	320	200

NUMERICAL MODEL

SORPAS®2D welding is used in this work for modelling approaches. Temperature dependent material properties of DP800, such as thermal conductivity, specific heat capacity, density, thermal expansion coefficient, Young's modulus, flow stress curves, were obtained from the SORPAS materials database. For welding simulation, a 1000Hz DC arbitrary projection/spot welding machine was selected from the SORPAS machine database and ISO5821 F1-16-20-6 CuCr1Zr electrodes with a geometry matching the experimental configuration were defined. Zinc surface coating was selected with a thickness of 50 g/m2. The model set-up for resistance spot welding is shown in Fig. 1. The numerical welding simulation in this work follows the ISO/TS 18166 guidelines [9].

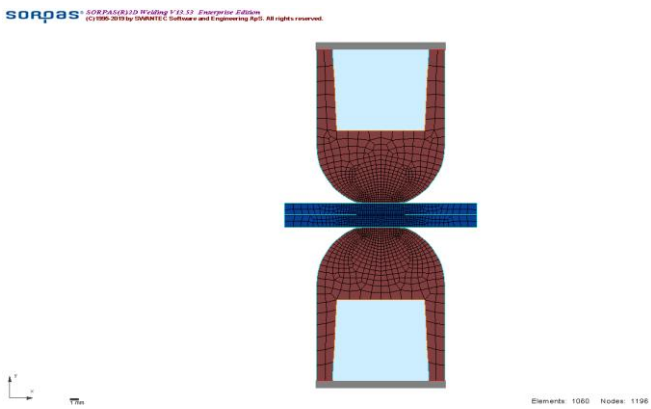

Fig. 1 Model set-up and mesh arrangement

ADVANCED ANALYTICAL MODEL

Advanced analytics employs predictive modeling, statistical methods, machine learning and process automation techniques beyond the capacities of traditional business intelligence (BI) tools to analyze data or business information. Three advanced analytical models were used in this study, i.e., multiple linear regression, decision tree and random forest. The scripts were compiled using Python language. Packages of SCIPY, PANDAS and NUMPY were imported.

Multiple linear regression (MLR) is a method used to model the linear relationship between a dependent variable and two or more independent variables. The MLR equation can be expressed as follows,

$$y = b_0 + b_1 x_1 + b_2 x_2 + ... + b_p x_p \quad (1)$$

where y is the predicted or expected value of the dependent variable, x_1 through x_p are p distinct independent or predictor variables, b_0 is the value of y when all the independent variables (x_1 through x_p) are equal to zero, and b_1 through b_p are the estimated regression coefficients. Each regression coefficient represents the change in y relative to a one-unit change in the respective independent variable. MLR is based on ordinary-least-squares (OLS), the model is fit such that the sum-of-squares of differences of observed and predicted values is minimized.

Decision tree builds regression or classification models in the form of a tree structure. It breaks down a dataset into smaller and smaller subsets while at the same time an associated decision tree is incrementally developed. The final result is a tree with decision nodes and leaf nodes. A decision node has two or more branches, each representing values for the attribute tested. Leaf node represents a decision on the numerical target. The topmost decision node in a tree which corresponds to the best predictor called root node. A node will be split if this split induces a decrease of the impurity greater than or equal to this value. The weighted impurity decrease equation is the following,

$$N\_t / N * (impurity - N\_t\_R / N\_t * right\_impurity - N\_t\_L / N\_t * left\_impurity) \quad (2)$$

where N is the total number of samples, N_t is the number of samples at the current node, N_t_L is the number of samples in the left child, and N_t_R is the number of samples in the right child. The advantages of decision trees are simple to understand and interpret and capable of handle both categorical and numerical data. However, a small change in the training data can result in a large change in the tree and consequently the final predictions.

Random forest is a model made up of many decision trees. Rather than just simply averaging the prediction of trees, this model uses two key concepts: random sampling of training data points when building trees and random subsets of features considered when splitting nodes.

RESULTS AND DISCUSSION

VALIDITY OF MATERIAL PROPERTIES AND NUMERICAL MODEL

The SORPAS material database provides properties of universal steel grades (*e.g.*, Mild steels, Dual phase steels, TRIP steels). DP800 was chosen in this work. In order to check the validity of the input material properties, chemical composition of the studied material from Table 1 was imported into JMatPro® to calculate the temperature dependent material properties, and then compared with those from the SORPAS materials database, as shown in Fig. 2. Reasonable agreements have been achieved for both the thermal conductivity and electrical resistivity. As temperature increases, the thermal conductivity from SORPAS database firstly increases to 35.4 W/ m K, and then decreases to 26.1 W/m K, and increases again at high temperatures up to 36.1 W/m K. The calculated thermal conductivity from JMatPro has a slightly overestimation in the temperature range from 300 to 1000 °C. For the electrical resistivity, it increases at elevated temperature. A very good agreement has been achieved between SORPAS and JMatPro. Thermal conductivity and electrical resistivity are the two most important properties for an electrical-thermal analysis, which determines the heat generation at the interfaces and the final weld nugget shape.

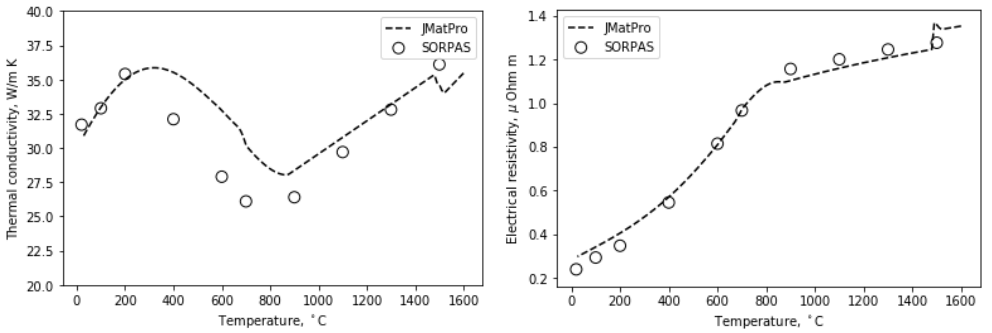

Fig. 2 Comparison of thermal conductivity (left) and electrical resistivity (right) from SORPAS and JMatPro

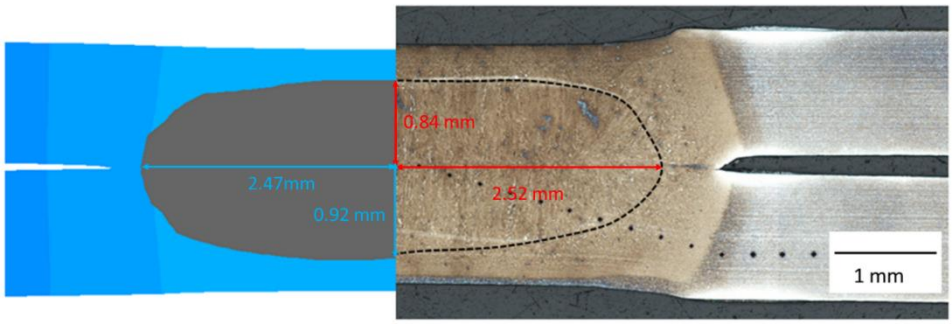

Fig. 3 Weld nugget size from numerical prediction and experiment measurement with welding current of 6 kA

The weld nugget size was used for validation of the numerical model. The welded sample was cut into cross-section and etched to visualize the weld fusion area. A comparison of the weld nuggets size with a welding current of 6 kA is shown in Fig. 3. A good agreement of the weld nugget shape between the experimental measurement and numerical prediction has been achieved.

ADVANCED ANALYTICS

After validation of the numerical model, in total 64 testing conditions were simulated considering different combinations of weld current (7-10 kA), squeeze force (3.5-5 kN) and weld time (280-400 ms). Hold time does not affect the nugget size and it is therefore not investigated. The simulated nugget diameter and height are listed in Table 3. It needs to be addressed that the “Height” exported from SORPAS output is half of the real nugget height. With the same force and time, diameter and height increase when current is increased. With the same force and current, diameter and height increase when time is increased. Increase either in time or current will increase the total heat input, and thus enlarge the nugget size. With the same time and current, diameter and height decrease when force is increased. Increase in force will increase the contact area and decrease the contact resistance at sheets interface. The total heat input is as a result decreased, and thus reduce the nugget size.

Table 3 Simulated weld nugget diameter and height with different combinations of squeeze force, weld time and weld current

Sample	Force (kN)	Time (ms)	Current (kA)	Diameter (mm)	Height (mm)
1	3.5	280	7	4.4237	0.70182
2	3.5	280	8	5.5245	0.89669
3	3.5	280	9	6.1294	0.94104
4	3.5	280	10	6.553	0.98001
5	4	280	7	4.1062	0.64227
6	4	280	8	5.2759	0.86884
7	4	280	9	6.0805	0.92618
8	4	280	10	6.5191	0.96463
9	4.5	280	7	3.9487	0.61293
10	4.5	280	8	5.1783	0.82468
11	4.5	280	9	6.06	0.91139
12	4.5	280	10	6.5057	0.95405
13	5	280	7	3.8082	0.55913
14	5	280	8	5.0542	0.77551
15	5	280	9	5.8206	0.89114
16	5	280	10	6.475	0.92805
17	3.5	320	7	4.6984	0.79285
18	3.5	320	8	5.6941	0.90322
19	3.5	320	9	6.2977	0.94355
20	3.5	320	10	6.7896	0.97874
21	4	320	7	4.5206	0.71044
22	4	320	8	5.6094	0.88946
23	4	320	9	6.202	0.92883
24	4	320	10	6.7442	0.96341
25	4.5	320	7	4.4326	0.68644
26	4.5	320	8	5.558	0.85753
27	4.5	320	9	6.1441	0.91349
28	4.5	320	10	6.7214	0.9525
29	5	320	7	4.0425	0.60017
30	5	320	8	5.3025	0.80125
31	5	320	9	6.1551	0.92083
32	5	320	10	6.6625	0.92901
33	3.5	360	7	5.0532	0.80764
34	3.5	360	8	5.8877	0.90686
35	3.5	360	9	6.3962	0.94257
36	3.5	360	10	6.9645	0.9772

37	4	360	7	4.8429	0.73625
38	4	360	8	5.8274	0.88872
39	4	360	9	6.3159	0.92887
40	4	360	10	6.9162	0.96132
41	4.5	360	7	4.6282	0.69027
42	4.5	360	8	5.7638	0.85777
43	4.5	360	9	6.3221	0.91415
44	4.5	360	10	6.8847	0.94867
45	5	360	7	4.3306	0.61704
46	5	360	8	5.5532	0.80036
47	5	360	9	6.2265	0.89761
48	5	360	10	6.746	0.92515
49	3.5	400	7	5.2071	0.8065
50	3.5	400	8	6.068	0.90581
51	3.5	400	9	6.587	0.94096
52	3.5	400	10	7.0357	0.96976
53	4	400	7	5.0281	0.73714
54	4	400	8	5.9915	0.88744
55	4	400	9	6.543	0.92703
56	4	400	10	7.0007	0.95227
57	4.5	400	7	4.883	0.69821
58	4.5	400	8	5.9304	0.8567
59	4.5	400	9	6.4763	0.91282
60	4.5	400	10	6.9718	0.93797
61	5	400	7	4.5363	0.63719
62	5	400	8	5.654	0.79939
63	5	400	9	6.3993	0.89579
64	5	400	10	6.9479	0.92291

The created database is divided into two sets, 70 % of which was used for training the model, and 30 % was kept for validation. Weld nugget diameter and height are defined as target functions. Three advanced analytical model were used, *i.e.*, multiple linear regression, decision tree and random forest. The associated results are shown in Fig. 4. A dashed line is plotted in every figure for reference. A shorter distance of the dots to the dashed line indicates a better fit of the predictions. R square (R^2) and root mean square error (RMSE) of the models are shown in Table 4. For nugget diameter prediction, the R^2 of the multiple linear regression model is 0.951 with a RMSE of 0.193 mm. Decision tree model shows a better prediction between 5.5 mm and 6.5 mm. The R^2 and RMSE are 0.973 and 0.141 mm respectively. Random forest model improves the prediction by random sampling the training points and random subset of features when splitting the nodes. The R^2 of random forest reaches 0.979 with a RMSE of 0.126 mm. For nugget

height prediction, the R^2 of multiple linear regression model only achieves 0.803, while decision tree and random forest have a better accuracy of 0.93 and 0.966, respectively.

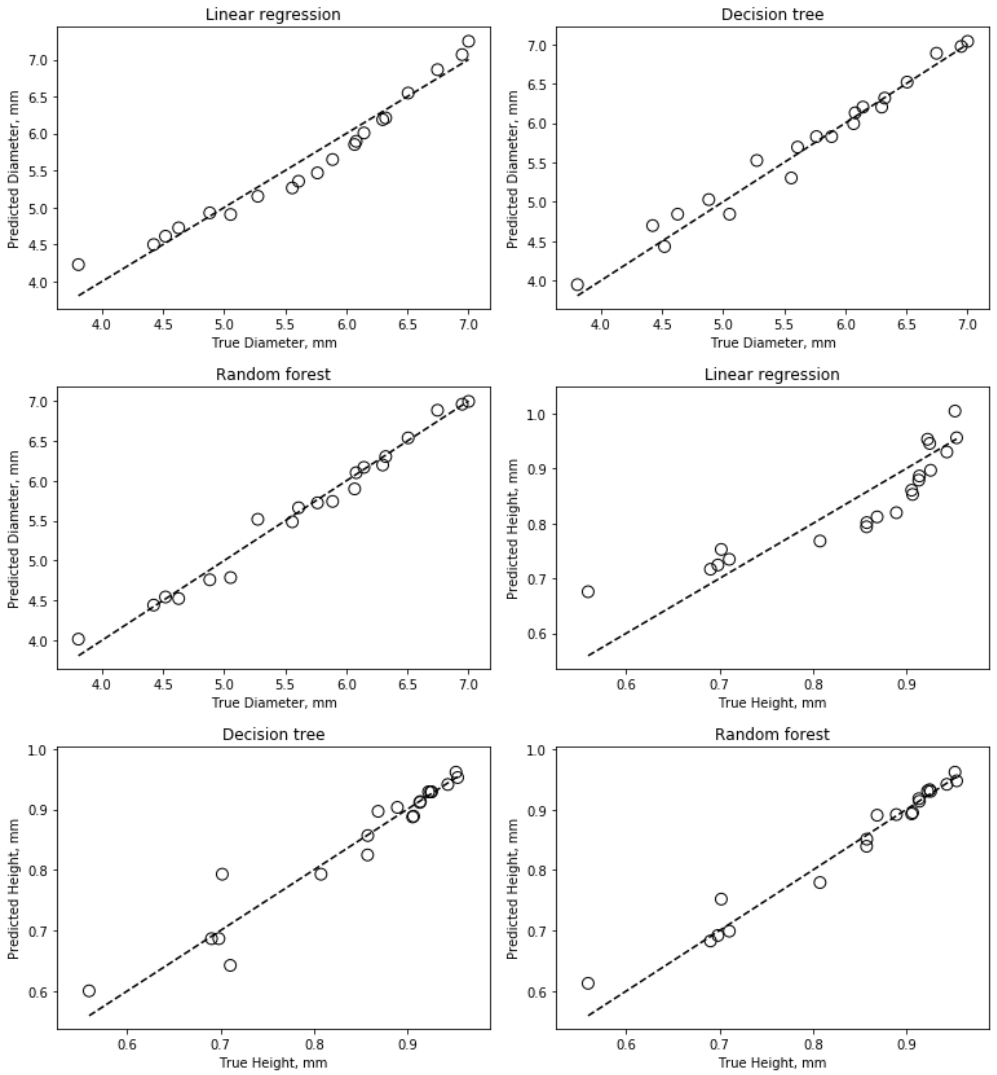

Fig. 4 Results of multi-linear regression, decisition tree and ranom forest models

Table 4 Results from different advanced analytical models.

	Linear regression	Decision tree	Random forest	Linear regression	Decision tree	Random forest
	Diameter			Height		
R^2	0.951	0.973	0.979	0.803	0.930	0.966
RMSE	0.193	0.141	0.126	0.048	0.028	0.019

Table 5 Weighting factors of decision tree and random forest models.

	Decision tree	Random forest	Decision tree	Random forest
	Diameter		Height	
Force	0.036	0.030	0.129	0.123
Time	0.065	0.062	0.021	0.020
Current	0.899	0.908	0.850	0.857

From the multiple linear regression model, three coefficients and one intercept of the input variables can be obtained. Therefore, a multi-linear equation can be generated to predict the weld nugget diameter and height based on force, time and current,

$$Diameter = -0.181 * force + 0.005 * time + 0.743 * current - 1.488 \quad (3)$$

$$Height = -0.051 * force + 0.0002 * time + 0.085 * current + 0.284 \quad (4)$$

Table 5 shows the weights of force, time and current related to nugget size. From the decision tree model, weld current is the dominating variable (more than 0.899) to determine the nugget diameter. Random forest model shows a slightly higher weight (0.908) than that of the decision tree. Weld time is ranked the second and squeeze force has the least influence on the nugget diameter. For prediction of nugget height, weld current has still the dominating weight of 0.85. However, squeeze force is ranked the second in the order of 0.12. Weld time has the least influence on the nugget height.

Besides ranking the weights of input variables, another advantage of using a tree-like model is to trace the split at every node. The 'sklearn.tree' package was used to export the data for node split. Fig. 5 shows the tree layout using 'Graphviz'. As 'current' has the most weight in determing the nugget size, it was picked as the root node. The threshold is 8.5 kA with 44 samples. The target value is 5.851 mm. 24 samples were found with 'current' greater than the first threshold. As there are many branches generated in the subsequent judgements, only the bottommost branch is chosen here for discussion. The second judgement is 'current' less than 9.5 kA, which returns 12 samples with 'truth' and 12 samples with 'false'. The third judgement is 'time' less than 300 ms, which returns 7 samples with 'truth' and 5 samples with 'false'. The fourth judgement is 'time' less than 380 ms, which returns 3 samples with 'truth' and 4 samples with 'false'. The fifth judgement is 'force less than 4 kN, which determines the weld diameter of 7.036 mm with 'truth' and 6.972 mm with 'false'. The similar interpretions can be applied to other branches.

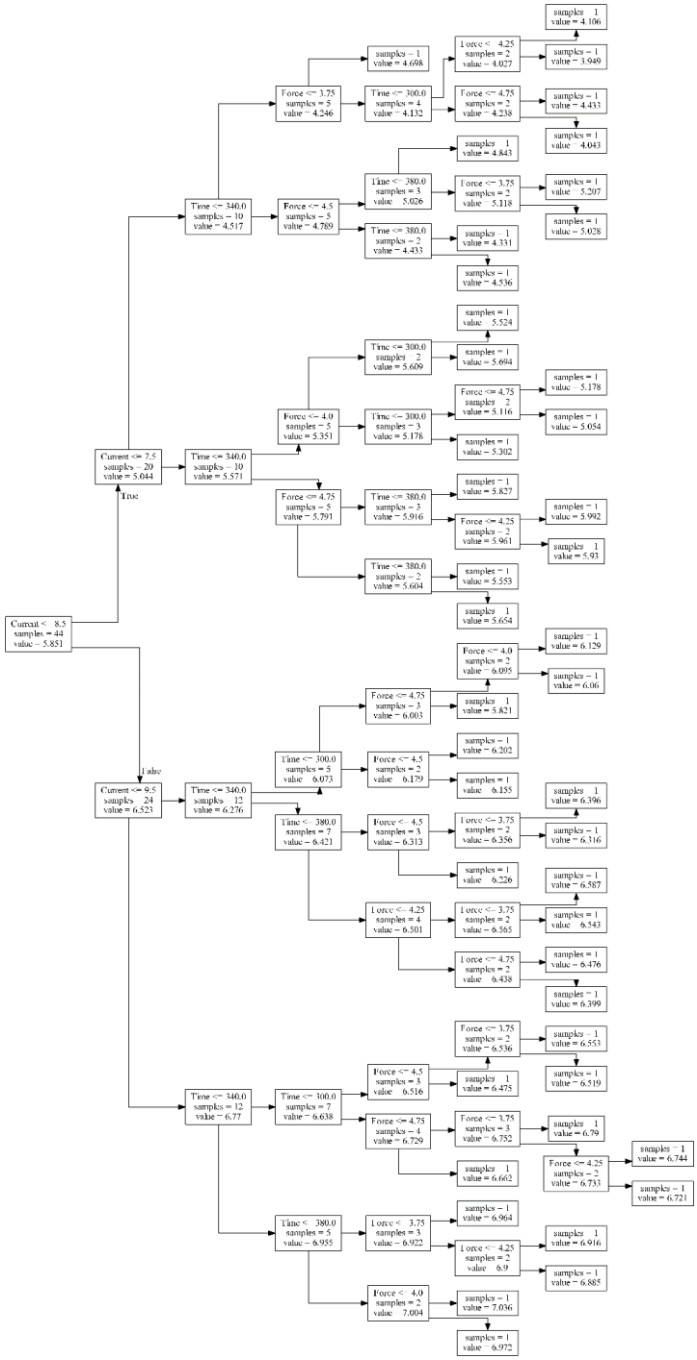

Fig. 5 Node split with respect to squeeze force, weld time and current

CONCLUDING REMARKS

In this work, finite element welding models are firstly validated with experimental measurements. Cases with different weld time, weld current and squeeze force are subsequently simulated in order to create a new database. Multiple linear regression, decision tree and random forest methods are used to train the analytical models. The trained analytical models are used to predict new experiments with reasonably good accuracy. In addition, weights for the input variables are explicitly ranked and discussed, which provides valuable information for optimizing the welding process. The main conclusions are summarized as follows,

- The approaches proposed in this work to combine the experiments, numerical models and analytical models are proven to be reliable and can be extended to other materials and processes.
- Increase in weld time or weld current, or decrease in squeeze force will increase the nugget size. With the studied material, multiple linear regression model provides two equations to calculate the nugget diameter and height with respect to weld time, weld current and squeeze force. Decision tree has a slightly better accuracy than multiple linear regression. Random forest provides the best predictions.
- Weld current has a dominating weight (more than 0.85) to determine the final nugget size. Squeeze force has a weight of 0.12 for determining the nugget height.

References

[1] W.J. JOOST: 'Reducing Vehicle Weight and Improving U.S. Energy Efficiency Using Integrated Computational Materials Engineering', *JOM 64*, 2012, pp. 1032-1038.

[2] M.P. MALI, K. INAMDAR: 'Effect of Spot Weld Position Variation on Quality of Automobile Sheet Metal Parts', *International Journal of Applied Research in Mechanical Engineering*, 2013, pp. 170-174.

[3] K. HEMMESI, M. FARAJIAN: 'Numerical Welding Simulation as a Basis for Structural Integrity Assessment of Structures: Microstructure and Residual Stresses', 2018, Article 74466.

[4] G. AGARWAL, A. KUMAR, I.M. RICHARDSON, M.J.M. HERMANS: 'Evaluation of solidification cracking susceptibility during laser welding in advanced high strength automotive steels', *Materials & Design*, Vol. 183, 2019, Article 108104.

[5] H. GAO, R.K. DUTTA, R.M. HUIZENGA, M. AMIRTHALINGAM, M.J.M. HERMANS, T. BUSLAPS, I.M. RICHARDSON: 'Pass-by-pass stress evolution in multipass welds', *Science and Technology of Welding and Joining*, Vol. 19, 2014, pp. 256-264.

[6] A. KUMAR, S. PANDA, G.K. GHOSH, R.K. PATEL: 'Numerical simulation of weld nugget in resistance spot welding process', *Materials Today: Proceedings*, Vol. 27, Part 3, 2020, pp. 2958-2963.

[7] W. GUAN, Y. ZHAO, Y. LIU, S. KANG, D. WANG, L. CUI: 'Force data-driven machine learning for defects in friction stir welding', *Scripta Materialia*, Vol. 217, 2022, Article 114765.

[8] *Stahl-Eisen-Prüfblätter Des Stahlinstituts VDEh*: 'Testing and Documentation Guideline for the Joinability of Steel Sheet Part 2: Resistance Spot Welding', 2008.
[9] ISO/TS 18166:2016 Numerical welding simulation - Execution and documentation.